Journal of Photochemistry and Photobiology A: Chemistry 216 (2010) 8–14

Contents lists available at ScienceDirect

Journal of Photochemistry and Photobiology A: Chemistry

journal homepage: www.elsevier.com/locate/jphotochem

All-solid-state electrolytes consisting of ionic liquid and carbon black for efficient dye-sensitized solar cells

Bing-Xin Lei, Wen-Jie Fang, Yuan-Fang Hou, Jin-Yun Liao, Dai-Bin Kuang*, Cheng-Yong Su

MOE Key Laboratory of Bioinorganic and Synthetic Chemistry, State Key Laboratory of Optoelectronic Materials and Technologies, School of Chemistry and Chemical Engineering, Sun Yat-Sen University, Guangzhou 510275, PR China

ARTICLE INFO

Article history:
Received 30 April 2010
Received in revised form 7 August 2010
Accepted 27 August 2010
Available online 28 September 2010

Keywords:
Dye-sensitized solar cell
Ionic liquid
All-solid-state electrolyte
Carbon black
TiO_2 nanocrystalline

ABSTRACT

All-solid-state electrolytes-based dye-sensitized solar cells (DSSCs) are constructed using a mixture of carbon black and 1-methyl-3-propylimidazolium iodide (PMII) ionic liquid without the addition of iodine, TiO_2/FTO glass, N719, and FTO glass as electrolyte, working electrode, light harvesting material and counter electrode, respectively. The influences of the electrolyte composition (weight ratio of carbon black and PMII), TiO_2 film thickness and the compact layer on the photovoltaic parameters of DSSCs have been investigated in detail. Electrochemical impedance spectroscopy (EIS) measurement is used to analyze the influence of electrolyte composition on the photovoltaic performance. The DSSC based on a 16.2 μm TiO_2 nanocrystalline film and an all-solid-state electrolytes containing 60 mg carbon black and 100 mg PMII exhibits a power conversion efficiency of 6.37%, short-circuit current density of 15.33 mA cm^{-2}, open-circuit voltage of 644 mV and fill factor of 64.5%, measured at AM 1.5 G one sun (100 mW cm^{-2}) illumination.

1. Introduction

Since the great breakthrough made by O'Regan and Grätzel, dye-sensitized solar cells (DSSCs) have attracted much attentions because of their high energy conversion efficiency and low production cost, making them a credible alternative to silicon solar cells [1]. Though the overall power conversion efficiency of more than 11% has been reported for DSSCs, which was based on a volatile liquid electrolyte as the hole-conducting element [2]. The liquid electrolytes-based DSSCs have the disadvantages of fluid, volatility, and electrode corrosion, which reduce the long-term stability and increase difficulties in sealing the device [3,4]. Recently, many efforts have been made to replace the liquid electrolytes with quasi-solid-state [5] or all-solid-state electrolytes [6], which have been the subject of intense study by various types of approaches using p-type inorganic semiconductors (CuI, CuSCN, etc.) [7–9], organic hole conductors [10–12], and gelator [13,14].

Pt deposited FTO glass was usually used as counter electrode for the I_3^- reduction because of its high catalytic activity, high conductivity, and stability. However, Pt is one of the most expensive components in DSSC. Therefore, development of inexpensive counter electrode materials to reduce production costs of DSSCs is much desirable. Several carbonaceous materials such as carbon nanotubes, activated carbon, graphite, and carbon black have been successfully employed as catalysts for the counter electrodes [15–20]. The results illustrated that carbonaceous materials not only gave ease in creating good physical contact with TiO_2 film but also functioned as efficient carrier collectors at the porous interface [21].

Recently, quasi-solid-state DSSCs based on polymer gel electrolyte with graphite powder or PEO/P(VDF-HFP)/SiO_2 nanocomposite polymer electrolyte with conductive carbon nanoparticles exhibited a power conversion efficiency of 3.25% or 4.27%, respectively [22,23]. Moreover, all-solid-state electrolytes containing polyaniline-loaded carbon black particles and an ethyleneoxide-substituted imidazolium iodide were developed for the DSSCs application, which showed overall conversion efficiencies of 3.48% and 4.07% for AM 1.5 G, 100 and 23 mW cm^{-2} irradiation, respectively [24]. These reported quasi-solid or all-solid-state electrolyte-based DSSCs used the Pt/FTO glass as counter electrode and the power conversion efficiencies were less than 5%. A higher efficiency of 6.15% has been recently reported for the quasi-solid-state DSSC which based on the mixture of binary ionic liquid and polyaniline-loaded carbon black [25]. Moreover, Pt/FTO glass was used as counter electrode.

In this article, a series of all-solid-state electrolytes were prepared by simply mixing 1-methyl-3-propylimidazolium iodide (PMII) and different amounts of carbon black. The present all-solid-state electrolytes contained carbon black, which can play catalytic effect and hence replace the expensive Pt. There are two obvious characteristics compared to the traditional DSSCs: (1) No addition of I_2 in the electrolytes to form I^-/I_3^- redox. A trace amount

---

* Corresponding author. Tel.: +86 20 84113015; fax: +86 20 84113015.
E-mail address: kuangdb@mail.sysu.edu.cn (D.-B. Kuang).

1010-6030/$ – see front matter © 2010 Elsevier B.V. All rights reserved.
doi:10.1016/j.jphotochem.2010.08.023

of iodine (I_2) was photochemically produced from ionic liquid at the photo-excited dye layer and involved in the redox reaction at the ionic liquid surface [24]. (2) No Pt loading on the FTO glass as counter electrode. DSSCs were fabricated by sandwiching the all-solid-state electrolytes between working electrode (dye adsorbed TiO_2/FTO glass) and counter electrode (bare FTO glass). Through the optimization of the electrolyte composition and TiO_2 nanocrystal film thickness, an overall solar to electric energy conversion efficiency of 6.37% was obtained for the all-solid-state DSSC, which is the best for the iodine-free solid-state DSSC.

2. Experimental

2.1. Materials

1-Methyl-3-propylimidazolium iodide (PMII), carbon black (Printex L, AG, average particle size 23 nm, Degussa), $[(C_4H_9)_4N]_2[Ru(II)L_2(NCS)_2]$, where L = 2,2′-bipyridyl-4, 4′-dicarboxylic acid (N719 dye, Solaronix SA, Switzerland), fluorine doped tin oxide glass (FTO glass, 14 Ω/□, 90% transmittance, Nippon Sheet Glass Co.).

2.2. Synthesis of anatase TiO_2 nanocrystalline powder

The precursor solution containing 15 mL $Ti(OBu)_4$ and 20 mL ethanol was magnetically stirred for 10 min at room temperature. Then, the precursor solution was added dropwise to a solution of 50 mL of acetic acid and 10 mL of deionized water under vigorous stirring for 1 h at room temperature. The mixture solution was transferred to a Teflon-lined stainless-steel autoclave and kept at 230 °C for 12 h, and then allowed to cool to room temperature naturally. Finally, the precipitation was filtered from the solution, washed with deionized water and ethanol several times to remove impurities, and dried in air at 50 °C for 6 h. The size of the TiO_2 nanoparticle is about 20 nm according to SEM and TEM measurements (data not shown). The synthesized TiO_2 nanocrystalline powder (1.0 g) was ground for 40 min in the mixture of ethanol (8.0 mL), acetic acid (0.2 mL), terpineol (3.0 g) and ethyl cellulose (0.5 g) to form a slurry, and then the slurry was sonicated for 5 min in an ultrasonic bath, finally to form a viscous white TiO_2 paste.

2.3. Preparation of quasi-solid-state and all-solid-state electrolytes

The mixture of 100 mg of PMII and different amounts of carbon black was ground to form homogeneous quasi-solid-state and all-solid-state electrolytes. The electrolytes were denoted as C1: 100 mg PMII + 15 mg carbon black, C2: 100 mg PMII + 30 mg carbon black, C3: 100 mg PMII + 45 mg carbon black, C4: 100 mg PMII + 60 mg carbon black, and C5: 100 mg PMII + 75 mg carbon black.

2.4. The assembly of the DSSCs

FTO conductive glass was firstly pre-coated with a TiO_2 compact layer of 200 nm thickness by spin coating a colloid solution (colloid size about 3–5 nm) to prevent a direct contact between the electrolytes and the FTO layer of conductive glass [26]. The TiO_2 colloid solution was synthesized based on a modified literature method [26,27]. Briefly, titanium n-butoxide (34.2 mL) was added slowly into a solution containing acetylacetone (10.2 mL) and n-butanol (37.6 mL) under stirring [26,27]. Hydrolysis of the clear mixture was then performed by the dropwise addition of an aqueous acidic solution (3.8 g paratoluenesulfonic acid in 18.0 mL H_2O). Stable transparent TiO_2 sol was obtained after heating the mixture solution at 60 °C for 12 h. The TiO_2 photoelectrodes were prepared via screen-printing of the above TiO_2 paste on the FTO glass substrate containing TiO_2 compact layer. The thickness of TiO_2 film can be adjusted via different times of screen-printing.

TiO_2 films were gradually heated under an air flow at 325 °C for 5 min, at 375 °C for 5 min, at 450 °C for 15 min, and then at 500 °C for 15 min. Then, TiO_2 films were soaked in 40 mM $TiCl_4$ aqueous solution for 30 min at 70 °C, which improved the photocurrent and photovoltaic performance of DSSCs. After treatment with $TiCl_4$, the TiO_2 films were rinsed with water and ethanol and then sintered at 520 °C for 30 min. After cooling to 80 °C, the $TiCl_4$ treated TiO_2 electrodes were immersed into the N719 dye solution (0.5 mM N719 in a mixture of acetonitrile and tert-butyl alcohol, 1:1 volume ratio) and then kept at room temperature for 16 h. The active area of the dye-coated TiO_2 film was 0.16 cm^2, which was measured by profilometer (Ambios, XP-1). The quasi-solid-state and all-solid-state electrolytes (C1–C5) were sandwiched between N719 sensitized TiO_2 film and a FTO glass (without Pt) under a certain pressure at room temperature.

2.5. Measurement and characterization

The electrolytes loaded TiO_2 films were characterized by field emission scanning electron microscope (FE-SEM, JSM-6330F) and energy dispersive spectroscopy (EDS, FEI/Quanta 400). The thicknesses of TiO_2 film were measured by using a profilometer (Ambios, XP-1) and SEM. The current–voltage characteristics were measured using a Keithley 2400 source meter under simulated AM 1.5 G illumination (100 mW cm^{-2}) provided by solar simulator (69920, 1 kW Xe lamp with optical filter, Oriel). The incident light intensity was calibrated with a NREL-calibrated Si solar cell. The electrochemical impedance spectroscopy (EIS) measurements were performed with a Zennium electrochemical workstation (ZAHNER) with the frequency range from 10 mHz to 1000 kHz. The magnitude of the alternative signal was 10 mV. The impedance measurements were carried out under forward bias of −0.65 V in the dark.

3. Results and discussion

3.1. Morphology of quasi-solid-state and all-solid-state electrolytes

The photographs of the quasi-solid-state and all-solid-state electrolytes containing 100 mg PMII ionic liquid and different amounts of carbon black are shown in Fig. 1. When adding 15 mg of carbon black into the 100 mg PMII, the electrolyte (C1) exhibited a dilute state or quasi-solid-state. With increasing carbon black content, the electrolytes (C2, 30 mg carbon black) became more viscous and all-solid-state (C3: 45 mg, and C4: 60 mg carbon black). Finally, for C5 electrolyte (75 mg carbon black), it looked like a clay.

Fig. 2 shows the FE-SEM images of the quasi-solid-state and all-solid-state electrolytes (C1 and C4) loaded into TiO_2 film. As shown in Fig. 2a, the FE-SEM image of top surface of C1 electrolyte/TiO_2 film exhibited a faint state due to a fewer amounts (15 mg) of carbon black. The cross-section (Fig. 2b) revealed that there was no obvious interface between the electrolyte and TiO_2 nanocrystalline layer because of the fluidity of the dilute electrolyte. However, for the electrolyte containing larger amount (60 mg) of carbon black, e.g. C4, the PMII ionic liquid was uniformly coated onto the carbon black surface, and formed a well-dispersed all-solid-state electrolytes (Fig. 2c, top surface of electrolyte/TiO_2 film). Clear interface between electrolyte and TiO_2 nanocrystalline layer is further observed (Fig. 2d, cross-section), revealing the formation of all-solid-state electrolytes. Moreover, both the quasi-solid-state (C1) and all-solid-state (C4) electrolytes were well-immersed into the voids of TiO_2 nanoparticles film, which was essential to the

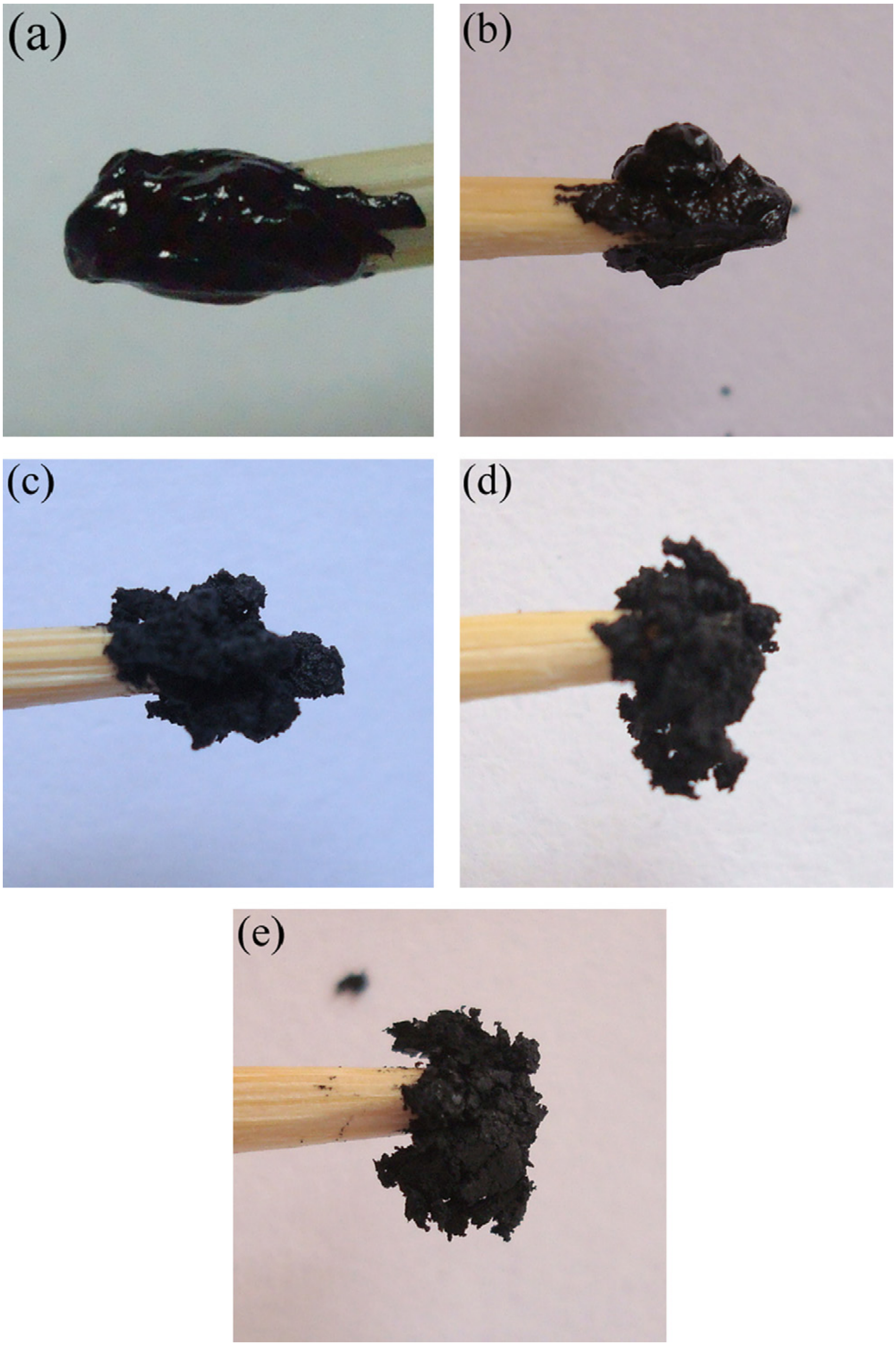

Fig. 1. Photographs of the quasi-solid-state and all-solid-state electrolytes containing 100 mg PMII and different amounts of carbon black. (a) C1, 15 mg; (b) C2, 30 mg; (c) C3, 45 mg; (d) C4, 60 mg; (e) C5, 75 mg.

higher photovoltaic performance of DSSCs. As shown in Fig. 2e, EDS data recorded from the area close to the FTO glass described the existence of the elements iodide and carbon, which revealed that the pores of the TiO_2 film were filled with the quasi-solid-state (C1) or all-solid-state (C4) electrolytes.

3.2. *Solar cell performance*

The present quasi-solid-state and all-solid-state dye-sensitized solar cells are constructed with N719 dye-sensitized TiO_2 film as working electrode, mixture of PMII and carbon black as electrolytes (C1–C5), and FTO glass as counter electrode. Fig. 3 shows the structure of solid-state electrolyte-based DSSC. In the present iodine-free solid-state electrolyte, the iodide based ionic liquid (PMII) provides sufficient I^- for the regeneration of the oxidized dye under light illumination (Eq. (1)), I^- simultaneously oxidizes to I_3^-, which can be reduced back to I^- at the electron transfer surface (PMII coated carbon black) (Eq. (2)):

$$3I^- + 2dye^+ \rightarrow I_3^- + 2dye \quad (\text{at dye/TiO}_2\ \text{interface}) \qquad (1)$$

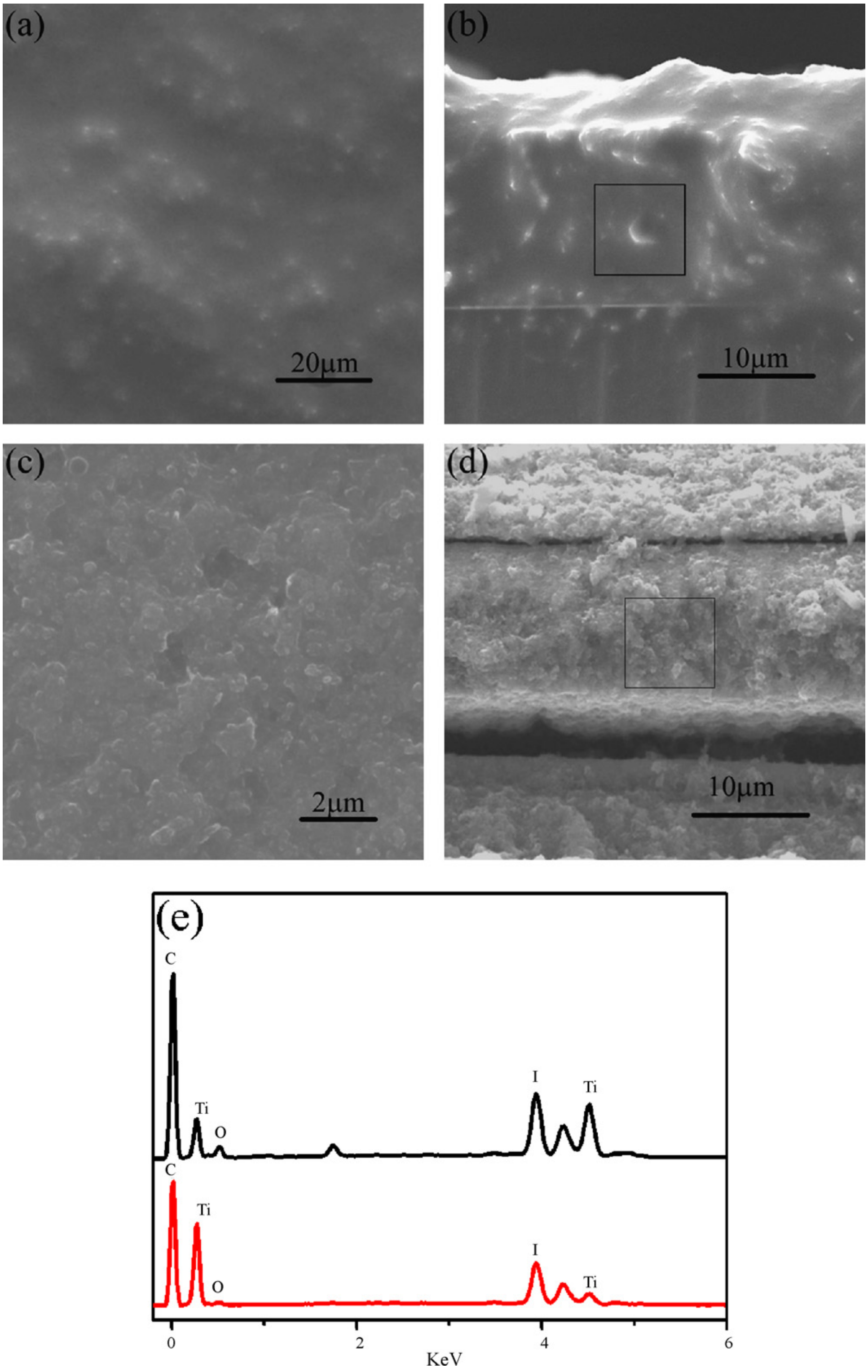

Fig. 2. FE-SEM images of the top surface of quasi-solid-state and solid-state electrolytes on the TiO_2 film – C1 (a) and C4 (c), and of the cross-section view – C1 (b) and C4 (d). (e) EDX spectra of the marked area in (b) (black curve, up curve) and (d) (red curve, down curve). (For interpretation of the references to color in this figure legend, the reader is referred to the web version of the article.)

$$I_3 + 2e^- \rightarrow 3I^- \quad \text{(at electron transfer interface)} \qquad (2)$$

The current density vs voltage curves of the DSSCs based on different quasi-solid-state and all-solid-state electrolytes (C1–C5) were measured under AM 1.5 G one sun (100 mW cm^{-2}) illumination. Fig. 4 shows the photocurrent–voltage characteristics of the quasi-solid-state and all-solid-state dye-sensitized solar cells and the corresponding open-circuit potential (V_{oc}), short-circuit current density (J_{sc}), fill factor (*FF*) and overall energy conversion efficiency (η) of these cells are summarized in Fig. 5. As shown in Figs. 4 and 5a, when the amount of carbon black increased from 15 to 60 mg, the J_{sc} and V_{oc} increased from 11.28 to 15.33 mA cm^{-2} and from 583 to 644 mV, respectively. The *FF* had a significant rise from 29% to 65%. Finally, the overall power conversion efficiency

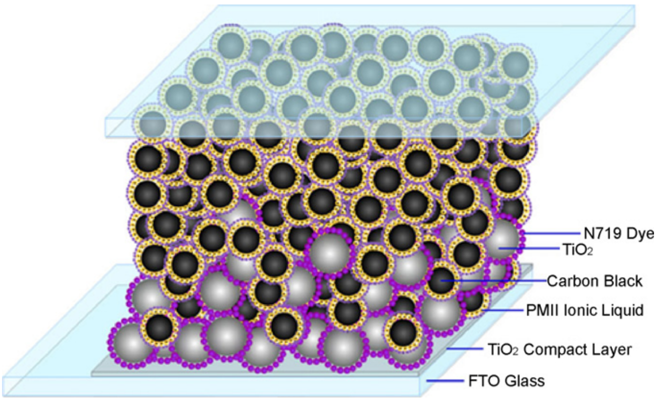

Fig. 3. Structure of the solid-state electrolytes-based dye-sensitized solar cell.

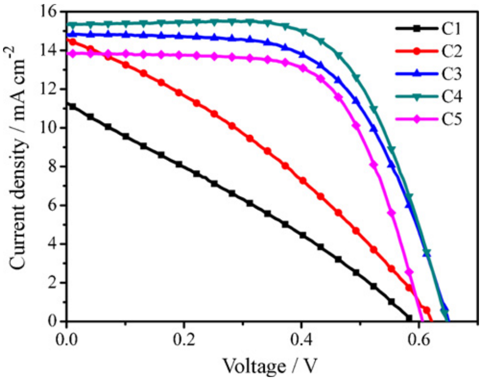

Fig. 4. Current density–voltage characteristics of dye-sensitized solar cells prepared with different quasi-solid-state and all-solid-state electrolytes (C1–C5) under AM 1.5 G one sun (100 mW cm^{-2}) illumination.

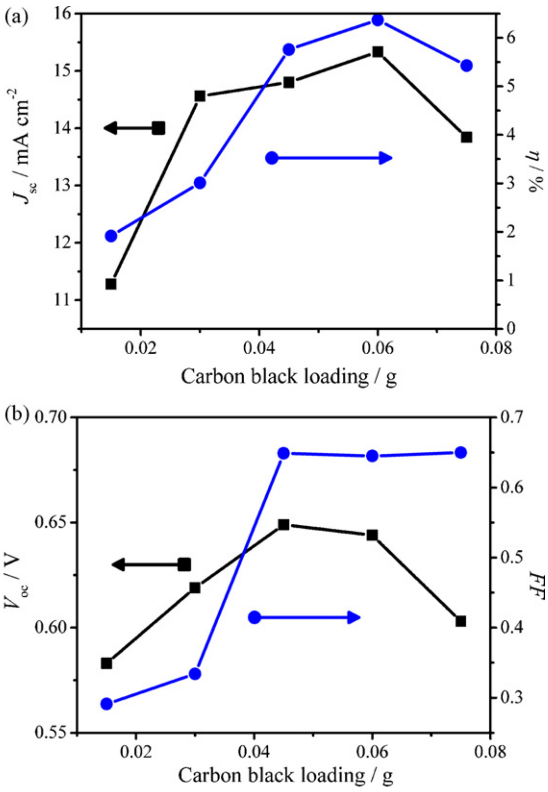

Fig. 5. (a) The short-circuit current density and power conversion efficiency of the DSSCs vs the carbon black content and (b) the open-circuit voltage and fill factor of DSSCs vs the carbon black content.

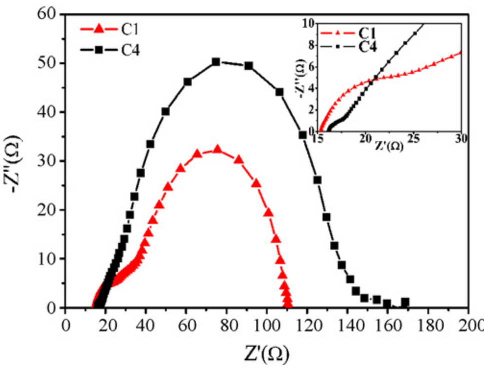

Fig. 6. Electrochemical impedance spectra (EIS) of the DSSCs with quasi-solid-state (C1) and all-solid-state electrolytes (C4), measured in darkness under −0.65 V applied bias. The inset is the enlarged part of high frequencies in the EIS.

increased from 1.92% to 6.37% with the increasing carbon black content. These results indicated that introduction of a slight amount of carbon black had a significant effect on the photovoltaic parameters (J_{sc}, V_{oc}, *FF*, and η). The increase of J_{sc} and V_{oc} with the increasing carbon black can be possibly attributed to the direct contact between dye/TiO_2 and I^-/I_3^- coated carbon black, which will improve the charge transportation or reduce the electron recombination. The higher conductivity and catalytic activities of the electrolyte with the increasing carbon black, and a zero distance between working electrode (TiO_2) and counter electrode (carbon black/FTO glass) for the present solar cell structure, both of which significantly reduce the internal resistance of the cell, are responsible for the enhancement of photovoltaic parameters [21]. The highest power conversion efficiency of 6.37% was obtained for the C4 electrolyte (100 mg PMII and 60 mg carbon black) with a V_{oc} of 644 mV, a *FF* of 64.5% and a J_{sc} of 15.33 mA cm^{-2}. However, further increase of the carbon black in the electrolyte, e.g. C5 (75 mg carbon black), the V_{oc}, J_{sc}, and η decreased, which can be possibly attributed to the poor penetration of the electrolyte into the porous TiO_2 electrode.

Electrochemical impedance spectroscopy (EIS) is used to elucidate the influences of the electrolyte composition on the photovoltaic performances of DSSCs. The Nyquist plots of the DSSCs based on the lowest efficiency electrolyte (C1) and the highest efficiency electrolyte (C4) are shown in Fig. 6. In general, three typical semicircles in the Nyquist plots are observed, which correspond to the I^-/I_3^- diffusion in the electrolyte, electron recombination at the TiO_2/electrolyte interface together with electron transport in the TiO_2 network, and charge transfer at the counter electrode in the order of increasing frequency [28]. However, in our experiment the conventional diffusion resistance of the redox couple is not observed due to a shorter length for I^- and I_3^- ions diffusion caused by the carbon material [25,29] at the electron transfer surface. The inset in Fig. 6 is the enlarged part of high frequency (the first semicircle). It clearly shows that the charge transfer resistance of C1 electrolyte at the counter electrode is larger than C4 electrolyte, which implies that the larger *FF* can be obtained for the C4 electrolyte compared to C1 electrolyte. Furthermore, at lower frequency (the second semicircle), smaller electron recombination resistance (at the TiO_2/electrolyte interface) is observed for DSSC based on C1 electrolyte compared to C4 electrolyte, implying a lower V_{oc} and/or J_{sc} for the former. These results are well in agreements with the above photovoltaic performances.

For comparison, DSSC (Fig. 7a) based on pure PMII ionic liquid electrolyte (without carbon black) showed a very poor photovoltaic performance (0.02%). This cell has no catalyst for the reduction of I_3^- [18,24], which is responsible for the lower J_{sc}, V_{oc}, *FF*, and η. Hence, the introduction of carbon black into the electrolyte is essential to the high photovoltaic performance. Furthermore, the effect

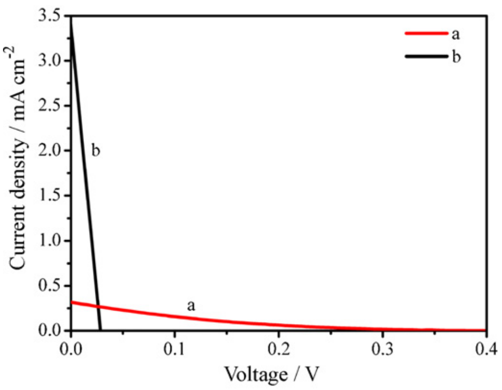

Fig. 7. (a) The photocurrent–voltage curve of DSSC based on an electrolyte with only PMII (without carbon black). (b) The photocurrent–voltage curve of the DSSC based on a working electrode without a TiO_2 compact layer.

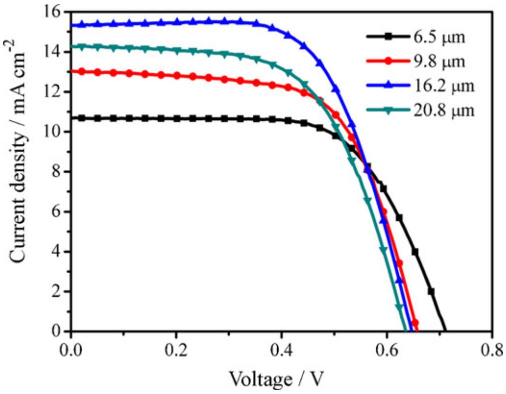

Fig. 8. The photocurrent–voltage curves of DSSCs based on different thicknesses of TiO_2 films and all-solid-state electrolyte (C4).

of compact layer on the photovoltaic performance was also investigated. Fig. 7b shows the photocurrent–voltage curve of the DSSC based on C4 electrolyte and TiO_2 film with 16.2 μm thickness in the absence of TiO_2 compact layer. The photovoltaic performance is only 0.024%, which is much lower than the above DSSC result (6.37%) with a TiO_2 compact layer. This can be possibly attributed to a direct contact between the conductive all-solid-state carbon black electrolytes and the conductive FTO substrate of the working electrode, which may form the short circuit, hence results in the poor photovoltaic performance. It shows that the TiO_2 compact layer is a prerequisite for the present all-solid-state dye-sensitized solar cells.

Furthermore, the influences of TiO_2 film thicknesses on the photovoltaic performance were further investigated. Fig. 8 shows the photocurrent–voltage curves of the DSSCs based on different TiO_2 film thicknesses with the C4 all-solid-state electrolytes measured under AM 1.5 G one sun (100 mW cm^{-2}) illumination. The detailed photovoltaic parameters (J_{sc}, V_{oc}, *FF*, and η) are summarized in Table 1. As shown in Fig. 8 and Table 1, the V_{oc} decreases from 648 to 606 mV with increasing film thickness from 6.5 to 20.8 μm, due to the augmentation of the surface area providing additional charge-recombination sites and enhancing the dark current [30]. Moreover, for thicker films the outer TiO_2 particle layers do not contribute significantly to the photogeneration of conduction band electrons due to the filtering of light by the dyed particles located close to the FTO glass. The sharing of photoinjected conduction band electrons by these particles lowers their quasi-Fermi level and hence the V_{oc} [30]. The J_{sc} increases from 10.68 to 15.33 mA cm^{-2} and then decreases to 14.28 mA cm^{-2} with the film thickness variation from 6.5, 16.2 to 20.8 μm. The initial increase of the J_{sc} can be attributed to the larger amounts of dye on the thicker TiO_2 film, and the decrease of the J_{sc} for 20.8 μm TiO_2 film can be ascribed to inefficient electron transportation in the TiO_2 film and poor penetration of the all-solid-state electrolytes into the porous thicker TiO_2. Hence, the optimal TiO_2 film thickness for the present all-solid-state dye-sensitized solar cell is 16.2 μm.

Table 1

Detailed photovoltaic parameters (J_{sc}, V_{oc}, *FF*, and η) of DSSCs based on different TiO_2 film thicknesses and C4 all-solid-state electrolytes.

Film thickness (μm)	J_{sc} (mA cm^{-2})	V_{oc} (mV)	*FF* (%)	η (%)
6.5	10.68	709	64.8	4.91
9.8	13.02	654	64.4	5.48
16.2	15.33	644	64.5	6.37
20.8	14.28	634	60.6	5.49

For comparison, a normal acetonitrile liquid electrolyte-based DSSC (16.2 μm in TiO_2 film thickness) was prepared, which shows a 12.98 mA cm^{-2}, 837 mV, 69% and 7.50% for J_{sc}, V_{oc}, *FF* and η, respectively. Though the photovoltaic performance of DSSCs based on the solid-state electrolyte (6.37%) is lower than that of the acetonitrile liquid electrolyte (7.50%), the stability test shows that the latter is better than the former. Without further sealing, after 1 week aging at room temperature, DSSCs based on the solid-state electrolyte keep 88% of initial photovoltaic performance, namely, from initial 6.37% decrease to 5.60%. However, the acetonitrile liquid electrolyte-based DSSCs drops dramatically, has only 33% of the initial value, namely, from initial 7.50% decreases to 2.51%. These results reveal the stability of the DSSC based on solid-state electrolyte is much better than that of acetonitrile liquid electrolyte.

4. Conclusion

In summary, dye-sensitized solar cell based on all-solid-state electrolytes consisting of PMII ionic liquid and carbon black showed a highly efficient power conversion efficiency of 6.37%, with a J_{sc} of 15.33 mA cm^{-2}, V_{oc} of 644 mV and *FF* of 64.5%. The photovoltaic parameters of the DSSCs were found to strongly depend on the carbon black content of the all-solid-state electrolytes and TiO_2 film thickness. Comparison experiments revealed that the addition of carbon black into the PMII and the TiO_2 compact layers on the FTO glass was crucial for the achievement of efficient photovoltaic performance.

Acknowledgements

The work was supported by the National Natural Science Foundation of China (20873183 and U0934003), the Natural Science Foundation of Guangdong Province (8151027501000030), the Open Foundation of the Key Laboratory of Enhanced Heat Transfer and Energy Conservation, Ministry of Education, Shenzhen Key Laboratory of Special Functional Materials (2T0806), Shenzhen University, Shenzhen, and the Foundation of Sun Yat-Sen University.

References

[1] B. O'Regan, M. Grätzel, A low-cost, high-efficiency solar cell based on dye-sensitized colloidal TiO_2 films, Nature 353 (1991) 737–740.
[2] M.K Nazeeruddin, F.D. Angelis, S. Fantacci, A. Selloni, G. Viscardi, P. Liska, S. Ito, B. Takeru, M. Grätzel, Combined experimental and DFT–TDDFT computational study of photoelectrochemical cell ruthenium sensitizers, J. Am. Chem. Soc. 127 (2005) 16835–16847.
[3] H.J. Snaith, L. Schmidt-Mende, Advances in liquid-electrolyte and solid-state dye-sensitized solar cells, Adv. Mater. 19 (2007) 3187–3200.
[4] C.S. Karthikeyan, H. Wietasch, M. Thelakkat, Highly efficient solid-state dye-sensitized TiO_2 solar cells using donor-antenna dyes capable of multistep charge-transfer cascades, Adv. Mater. 19 (2007) 1091–1095.
[5] E. Stathatos, Y.J. Chen, D.D. Dionysiou, Quasi-solid-state dye-sensitized solar cells employing nanocrystalline TiO_2 films made at low temperature, Sol. Energy Mater. Sol. Cells 92 (2008) 1358–1365.

[6] R. Kawano, T. Katakabe, H. Shimosawa, M.K. Nazeeruddin, M. Grätzel, H. Matsui, T. Kitamura, N. Tanabe, M. Watanabe, Solid-state dye-sensitized solar cells using polymerized ionic liquid electrolyte with platinum-free counter electrode, Phys. Chem. Chem. Phys. 12 (2010) 1916–1921.

[7] V.P.S. Perera, P.K.D.D.P. Pitigala, P.V.V. Jayaweera, K.M.P. Bandaranayake, K. Tennakone, Dye-sensitized solid-state photovoltaic cells based on dye multilayer-semiconductor nanostructures, J. Phys. Chem. B 107 (2003) 13758–13761.

[8] G.R.A. Kumara, A. Konno, K. Shiratsuchi, J. Tsukahara, K. Tennakone, Dye-sensitized solid-state solar cells: use of crystal growth inhibitors for deposition of the hole collector, Chem. Mater. 14 (2002) 954–955.

[9] Q.B. Meng, K. Takahashi, X.T. Zhang, I. Sutanto, T.N. Rao, O. Sato, A. Fujishima, H. Watanabe, T. Nakamori, M. Uragami, Fabrication of an efficient solid-state dye-sensitized solar cell, Langmuir 19 (2003) 3572–3574.

[10] U. Bach, D. Lupo, P. Comte, J.E. Moser, F. Weissortel, J. Salbeck, H. Spreitzer, M. Grätzel, Solid-state dye-sensitized mesoporous TiO_2 solar cells with high photon-to-electron conversion efficiencies, Nature 395 (1998) 583–585.

[11] J. Kruger, R. Plass, L. Cevey, M. Piccirelli, M. Grätzel, U. Bach, High efficiency solid-state photovoltaic device due to inhibition of interface charge recombination, Appl. Phys. Lett. 79 (2001) 2085–2087.

[12] J. Kruger, R. Plass, M. Grätzel, H.J. Matthieu, Improvement of the photovoltaic performance of solid-state dye-sensitized device by silver complexation of the sensitizer cis-bis(4,4′-dicarboxy-2,2′ bipyridine)-bis(isothiocyanato) ruthenium(II), Appl. Phys. Lett. 81 (2002) 367–369.

[13] N. Mohmeyer, D.B. Kuang, P. Wang, H.W. Schmidt, S.M. Zakeeruddin, M. Grätzel, An efficient organogelator for ionic liquids to prepare stable quasi-solid-state dye-sensitized solar cells, J. Mater. Chem. 16 (2006) 2978–2983.

[14] W. Kubo, K. Murakoshi, T. Kitamura, S. Yoshida, M. Haruki, K. Hanabusa, H. Shirai, Y. Wada, S. Yanagida, Quasi-solid-state dye-sensitized TiO_2 solar cells: effective charge transport in mesoporous space filled with gel electrolytes containing iodide and iodine, J. Phys. Chem. B 105 (2001) 12809–12815.

[15] T.N. Murakami, S. Ito, Q. Wang, M.K. Nazeeruddin, T. Bessho, I. Cesar, P. Liska, R. Humphry-Baker, P. Comte, P. Pechy, M. Grätzel, Highly efficient dye-sensitized solar cells based on carbon black counter electrodes, J. Electrochem. Soc. 153 (2006) A2255–A2261.

[16] Z. Huang, X.H. Liu, K.X. Li, D.M. Li, Y.H. Luo, H. Li, W.B. Song, L.Q. Chen, Q.B. Meng, Application of carbon materials as counter electrodes of dye-sensitized solar cells, Electrochem. Commun. 9 (2007) 596–598.

[17] K. Suzuki, M. Yamaguchi, M. Kumagai, S. Yanagida, Application of carbon nanotubes to counter electrodes of dye-sensitized solar cells, Chem. Lett. 32 (2003) 28–29.

[18] G.Q. Wang, W. Xing, S.P. Zhuo, Application of mesoporous carbon to counter electrode for dye-sensitized solar cells, J. Power Sources 194 (2009) 568–573.

[19] W.J. Lee, E. Ramasamy, D.Y. Lee, J.S. Song, Performance variation of carbon counter electrode based dye-sensitized solar cell, Sol. Energy Mater. Sol. Cells 92 (2008) 814–818.

[20] S.I. Cha, B.K. Koo, S.H. Seo, D.Y. Lee, Pt-free transparent counter electrodes for dye-sensitized solar cells prepared from carbon nanotube micro-balls, J. Mater. Chem. 20 (2010) 659–662.

[21] T. Miyasaka, N. Ikeda, T.N. Murakami, K. Teshima, Light energy conversion and storage with soft carbonaceous materials that solidify mesoscopic electrochemical interfaces, Chem. Lett. 36 (2007) 480–487.

[22] Q.H. Li, J.H. Wu, Q.W. Tang, Z. Lan, P.J. Li, T.T. Zhang, Application of polymer gel electrolyte with graphite powder in quasi-solid-state dye-sensitized solar cells, Polym. Compos. 30 (2009) 1687–1692.

[23] J. Zhang, H.W. Han, S.J. Wu, S. Xu, Y. Yang, C.H. Zhou, X.Z. Zhao, Conductive carbon nanoparticles hybrid PEO/P(VDF-HFP)/SiO_2 nanocomposite polymer electrolyte type dye sensitized solar cells, Solid State Ionics 178 (2007) 1595–1601.

[24] N. Ikeda, K. Teshima, T. Miyasaka, Conductive polymer–carbon–imidazolium composite: a simple means for constructing solid-state dye-sensitized solar cells, Chem. Commun. (2006) 1733–1735.

[25] P.Y. Chen, C.P. Lee, R. Vittal, K.C. Ho, A quasi solid-state dye-sensitized solar cell containing binary ionic liquid and polyaniline-loaded carbon black, J. Power Sources 195 (2010) 3933–3938.

[26] Y.F. Wang, J.W. Li, Y.F. Hou, X.Y. Yu, C.Y. Su, D.B. Kuang, Hierarchial tin oxide octahedra for highly efficient dye-sensitized solar cells, Chem. Eur. J. 16 (2010) 8620–8625.

[27] E. Scolan, C. Sanchez, Synthesis and characterization of surface-protected nanocrystalline titania particles, Chem. Mater. 10 (1998) 3217–3223.

[28] D.B. Kuang, C. Klein, Z.P. Zhang, S. Ito, J.E. Moser, S.M. Zakeeruddin, M. Grätzel, Stable, high-efficiency ionic-liquid-based mesoscopic dye-sensitized solar cells, Small 3 (2007) 2094–2102.

[29] C.P Lee, P.Y. Chen, R. Vittal, K.C. Ho, Iodine-free high efficient quasi solid-state dye-sensitized solar cell containing ionic liquid and polyaniline-loaded carbon black, J. Mater. Chem. 20 (2010) 2356–2361.

[30] D.B. Kuang, S. Ito, B. Wenger, C. Klein, J.E. Moser, R. Humphry-Baker, S.M. Zakeeruddin, M. Grätzel, High molar extinction coefficient heteroleptic ruthenium complexes for thin film dye-sensitized solar cells, J. Am. Chem. Soc. 128 (2006) 4146–4154.